ASTES

Advances in Science, Technology and Engineering Systems Journal Vol. 9, No. 1, 149-164 (2024)

www.astesj.com

ASTESJ

ISSN: 2415-6698

Development of a GSM-RC Automated Device for Measuring Mobile Communication Signal Strength and Meteorological Parameters

Giwa Abdulgafar Babatunde[1], Ewetumo Theophilus[1], Ojo Joseph. Sunday[1*], Adedayo Kayode David[1], Owolabi Gbenga Ayodele[2]

[1]*Department of Physics, Federal University of Technology Akure, 2340001, Nigeria*

[2] *Engineering and Maintenance Unit, NNPC Retail Ltd, Abuja, Nigeria*

ARTICLE INFO

Article history:
Received: 13 December, 2023
Revised: 27 January, 2024
Accepted: 28 January, 2024
Online: 21 February, 2024

Keywords:
GSM-RC Device
GSM received signal strength
Meteorological parameters
Field test

ABSTRACT

The automated Global System for Mobile Communication Signal Strength and Radio Climatological (GSM-RC) measuring device is an integration of different electronic sensors in a box for an in-situ measuring system. The sensor, data logging, and communication subsystems are integrated for transmitting information on meteorological parameters (MPs) and GSM signal strength level (SSL). The goal is to develop a device that could simultaneously measure MP and SSL of GSM communication systems in any location of interest. This is to reduce significant errors due to a lack of synchronization among multiple devices. To accomplish this objective, we designed an atmospheric sensing system with GSM SSL, temperature, relative humidity, and pressure sensors integrated as a GSM-RC unit. An Arduino microcontroller unit was used to wirelessly transmit the data collected by various sensors in each subsystem and stored on a micro-SD card. A statistical analysis of the SSL between the GSM-RC and the Samsung Galaxy A10s mobile reveals a correlation of roughly 0.99. The ANOVA analysis of variance demonstrates no noticeable distinction between the SSL from developed and conventional devices. The P-value is about 0.93, with α-value of 0.05. The MPs were validated with a standard Vintage Pro weather station, and the data were statistically correlated with accuracies close to unity. A field test was carried out with the device to measure the SSL through the GSM and the selected MP in Akure from January to December 2022. The findings indicate a weak and poor correlation between temperature and signal strength, while relative humidity and pressure have a positive and weak correlations with the signal strength. This implies that an increase in SSL leads to a slight decrease in temperature while the relative humidity and pressure increase slightly. Other than being affordable in terms of production and deployment, the device has also solved the problem of labour-intensiveness arising from bulkiness.

1. Introduction

Over the years, when considering the impact of meteorological parameters (rain, temperature, pressure, relative humidity, etc.) on the received signal strength (RSS), scientists usually carried out research based on modeling and in-situ measurement of the meteorological parameter using separate devices for measurements [1]. Among the devices that can measure some of these parameters, there are both fixed and mobile types. Examples of such devices are the automatic weather station, Vintage Pro and Vantage Vue, and divers of rain gauges, among others. However, studies show that most of these equipments are expensive and bulky, and the results have always led to significant errors due to a lack of synchronization [2-3]. RSS is also measured with a signal strength meter, a signal strength application installed on mobile phones, SATlink, and a field strength meter. In order to give room for synchronization, there is a need to develop a device that will address the aforementioned drawbacks in accounting for the exact and concurrent measurements of the GSM signal strengths and meteorological parameters.

The act of measuring involves expressing the relationship between two quantities that are directly accessible to the terminal element of measuring equipment. Electrical signals can be obtained directly when a variation of an intermediate quantity causes some modification of the intense qualities of the sensitive device, or indirectly when a physical quantity, such as speed, heat, etc., generates an electrical quantity, such as in thermo-electricity-conductivity, permeability, and permittivity [4]. Electronic methods, whose benefits are numerous and unquestionable, have

*Corresponding Author: Ojo Joseph. Sunday, Department of Physics Federal University of Technology Akure, Nigeria, & ojojs_74@futa.edu.ng

made measuring electrical signals simple. It is necessary to determine the quantities of electrical values using the proper measuring device. These tools enhance or add to human sense-making, perception, calculation, and evaluation abilities. The transducer, whose main purpose is to convert some physical variables to electrical variables, is one of the key components in this regard [4]. The current communication systems face challenges from the quest for ubiquitous connectivity due to some physical restrictions. Also, customers demanded their service providers to deliver good quality services. Therefore, systems that can be swiftly implemented and offer bandwidth-efficient communications must be produced by manufacturers. Instrumentation and measurements serve a crucial and essential part in achieving this goal [5] Rigid testing is carried out throughout the early stage of equipment development to evaluate system functioning and performance as well as to guarantee system interoperability. Additionally, the complexity of communication signals is putting additional stress on design teams, which already have a lot of work to do. The developer must not only conduct conformance testing but also swiftly determine the underlying reasons for potential technical issues using measurement results.

To properly emphasize the importance of measurement, it is helpful to refer to a common and well-known wireless communication system that uses radio frequency –RF [5]. The signal strength metre, also referred to as an electromagnetic radiation tester, is a special receiver designed to gauge the electromagnetic wave (EM wave) strength emitted by any transmitter operating within the same frequency bands and to show the output on a regulated scale, liquid crystal display (LCD) or light-emitting diode (LED) monitored [6]. The amount of carrier wave modulation and antenna directivity, the distance between the points of reception and transmission, the attenuation the signal experiences as it travels between the two points, the strength of interference at the receiving end, the fading caused by direct and indirect signals, and the quality of the signal are all factors needed for the ability of a signal strength meter to receive a satisfactory signal from a given broadcasting station at any given point [4].

Given the significance and complexity of electromagnetic waves, such as the frequency-modulated signal (FM signal), there is a need for a direct measuring device to identify their presence and strength. This would enable designers and technicians to evaluate transmitter performance and predict their projected range. Making a field test is one method of obtaining this conclusion, although this sometimes requires moving across different distances with a radio receiver and comparing attenuation levels. According to technical literature, a communication system is a setup made up of physical structures, various types of equipment (transmitters, receivers, and repeaters), and different add-ons or enhancements (encryption, security solutions, and interoperability or networking), intending to disseminate information following user needs. Each component must have a single goal, work together technically, follow similar practices, react to controls, and generally operate in harmony [7] .

The majority of wireless localization systems employ either timing information or features of the received signal to estimate the distance to the positioning beacons, with RSSI being the most often used signal-related aspect. However, RSSI data are not always available from the hardware, or they are supplied with very low granularity, limiting the positioning system's accuracy. Other signal properties could be employed to estimate the distance between the mobile unit and the positioning beacons to solve this problem [8]. Simulation techniques, empirical models, deterministic models, theoretical models, and stochastic models have all been used to study GSM signal strength and some weather parameters. However, these existing methods have flaws in accounting for exact and concurrent measurements of weather parameters and propagated GSM signal strength with the same real-time synchronizations. As a result of the need to address the aforementioned flaw, a GSM signal strength and radio climatological measuring device was developed to evaluate the quality of specific signal strength and instantaneous climatological parameters.

The loss in signal strength of a GSM signal should not be overlooked because it has a significant impact on the quality of the call received. Because some of the available devices could not account for both real-time and concurrent measurements of the signal strength under meteorological conditions, individual measurements of the parameters were used instead. To solve the aforementioned shortcomings, a portable, easy-to-repair, low-cost, and easy-to-deploy GSM signal strength and radio climatological measurement device is the goal of this work. The developed device will replace the time-consuming and inconvenient methods of measuring GSM signal strength and radio-climatological parameters individually.

2. Method and Materials

The goal of this study is to develop a cheap, miniaturized, and efficient device that simultaneously measures atmospheric parameters and received signal strength (RSS). In this section, an outline of the necessary hardware and software used in developing the GSM-RC automated device is highlighted. The hardware section analyzes in detail the mode of selection of various sensors, while the software section highlights the Arduino integrated development environment (IDE) and other software tools used during the design. Furthermore, the data collection procedures and field tests using the developed device are also presented. Figure 1 presents a block diagram of the design and operation of the automated GSM-RC device

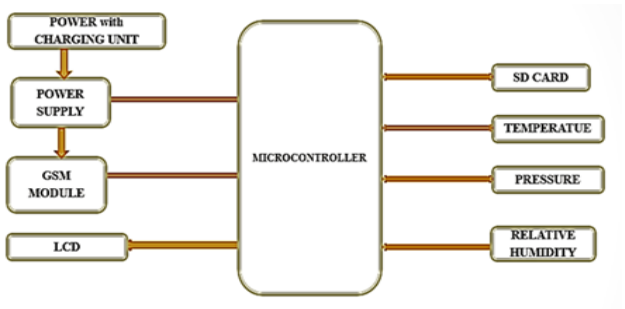

Figure 1: Systematic block diagram representation of the methodology adopted

2.1. GSM-RC major subsystem

The automated GSM-RC is composed of three main sections: the communication subsystem, the data logging subsystem, and the sensors subsystem. The sections cover the various components of each subsystem. The discussion is focused on how the components

used in this study function and operate. The GSM-RC assembly process is shown in Figure 2.

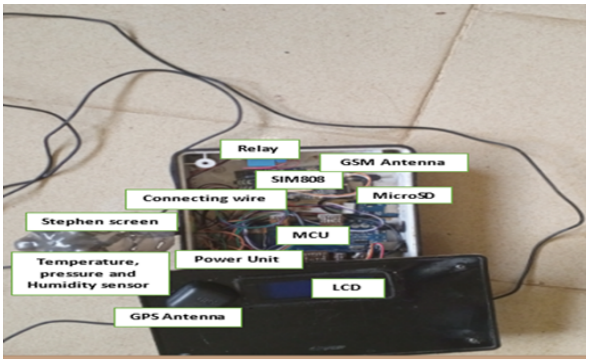

Figure 2: Assembly stage of the GSM-RC

2.2. Sensor subsystem

This system is made up of locally available electronic sensors that access physical features such as temperature, humidity, pressure, and GSM signal strength. The BME280 is a temperature sensor categorized as an integrated silicon temperature sensor. It is based on piezo-resistive technology, which has a semiconducting material (usually silicon) that changes the resistance when a mechanical force like atmospheric pressure is applied and can be integrated into the system over the inter-integrated circuit (I2C) interface. It has a ± 2 ℃ accurate analog output temperature sensor with an operating voltage range of 3 V to 5 V and a wide temperature range of – 40 ℃ to + 85 ℃. Also known as a pressure sensor, it acts as a transducer, generating an output signal as a function of pressure. It has a measuring range between 300 hPa and 1100 hPa. The HTU31 is a humidity sensor with an analog-output integrated circuit. It uses a laser-trimmed, thermoset polymer capacitive sensing element with on-chip integrated signal conditioning.

2.3. Data logging and Communication Subsystem

While the communication system assures reliable data transmission to the storage device, the data logging system enables accurate data collection, organization, transmission, and processing. This subsystem integrates a number of components to make the device conform to a normal mobile station and complete the required task. There is a SIM808 module that is integrated with a high-performance GSM/GPRS engine, a GPS engine, and a Bluetooth engine. SIM808 is a quad-band GSM/GPRS module that works on frequencies 850 MHz (GSM), 900 MHz (EGSM), 1800 MHz (DCS), and 1900 MHz (PCS), thereby obtaining the Received Signal Strength of the GSM-RC with respect to the network's frequency. In case the communication links stop, a microSD card module is provided as a storage device. The measured data can be kept on the micro-SD card for later analysis because radio signals can be easily interfered with during undesirable weather conditions, rendering transmission null [9]. At such times, there may be trouble with transmission to the ground station. All the components in the major subsystems' output data are in quantitative form and need to be analyzed. This is accomplished by using an Arduino ATmega 2560 microcontroller to wirelessly transmit the data collected by various sensors in each subsystem. During the SIM808's mission, this microcontroller creates the communication link between the SIM808 and the base transceiver station. Real-time data processing and archiving are made feasible by the microcontroller that receives the data. Individually and with the aid of the Arduino IDE software, these modules and the circuits that go with them were created and tested. Following the implementation of the circuits, inferences might be made using the stored data.

2.4. Power sizing

The most accurate way for determining how much power is utilized by each component in various subsystems is power sizing. Making plans for the type of battery to utilise is made easier with this knowledge [10]. The formula P = IV, where P is the electric power in Watts, V is the voltage differential in Volts, and I is the current in mA, was used to extract data on power consumption for each component from multiple data sheets. The data obtained in Table 1 guides us in choosing the right battery to be used by the automated GSM-RC device subsystems. Another factor is the weight of the device, in that the battery chosen should be light.

Table 1: Voltage, current and power ratings of various components of the GSM-RC

Components	Voltage (V)	Current (mA)	Power (mW)
Arduino	5.0	20.0	100.00
GSM Module	12.0	44.0	528.00
Relay	5.0	20.0	100.00
HTU31	5.0	1.0	5.00
BME280	3.3	0.6	1.98
SD Card Shield	3.3	5.0	16.50
Total Power		90.6	751.48

2.5. Software design and programming

The Arduino IDE is a piece of open-source software used to code the Arduino ATmega board. Using the C and C++ programming languages, this software makes it simple to develop instructions to programme the various sensors. An onboard computer, or microcontroller, such as an Arduino board, takes input and transforms the input signal into a readable output. The primary logical decisions related to the instructions given by the Arduino IDE software are made by this microcontroller. The board has been coded to read and interpret the values of the sensor outputs. The processed data from these sensors will be displayed on the liquid crystal display as digital values.

2.6. Testing

Boiling water in a kettle on the stove produced a humid environment. Because of the abundant steam that is released into the air, the humidity has increased. As soon as water hits the boiling point, it starts to emit steam and re-evaporate back into the atmosphere. The sensor was placed in a humid environment to monitor its measurement, and the humidity level increased with time. The temperature value recorded by the temperature sensor drops to that of room temperature when it is moved away from the heat source. The temperature rises as it gets closer to the heat source. The microcontroller and SIM808 modules' LEDs light red when the power is turned on. When the sensing signal LED starts flashing, the module detector is pressed and held in place before being released, and launching a search for data requires more than 3 minutes. Thus, all exhibit appropriate behavior in their responses.

3. Results and Discussion

In this section, a number of data sets that were collected from the in-situ measurements of the automated GSM-RC are illustrated graphically and in Table format..

3.1. Data from field test

The device was deployed to the field to ascertain the status of the real-time measurement. Table 2 presents a sample of a typical measurement on the field. Although not shown in Table 2, the measured result shows that the device can successfully measure the GSM signal strength up to -165 dBm and the selected radio climatological parameters [temperature (°C), humidity (%), and pressure (mbar)]. The device was also capable of measuring the number of base stations and both satellites in view and in operation. The logging time was rapid, with a response time of 30 seconds or less. The temperature sensor in use measures temperature with a resolution of 0.25 °C between -40 °C and 85 °C, and its maximum humidity range is about 99%..

3.2. Validating the device measurement with an existing equipment

The data obtained was validated with the existing equipment. A Vantage Vue Integrated Sensor Suite (ISS) has been installed at the Physics Department, Federal University of Technology Akure, Nigeria. The equipment measures, among others, meteorological parameters such as temperature, pressure, and relative humidity. They were measured with the DAVIS Vantage Vue Integrated Sensor Suite (ISS) weather station at 1- minute integration time and co-located with the developed device. The data were respectively stored in the data loggers of both the developed and the DAVIS Vantage Vue Integrated Sensor Suite (ISS) weather station devices, from where they were downloaded and extracted. For performance purposes, the sensor temperature, relative humidity, and pressure of the developed device were enclosed in a prototype Stephen screen against precipitation and direct heat radiation from outside sources while still allowing air to circulate freely around them. This is done to validate the accuracy of the sensors. The responses obtained are presented in Figures 3–5 for temperature, relative humidity, and pressure, respectively. The characteristic equations obtained for each of the parameters were shown in equations (1) – (3), respectively:

For Temperature (BME280),

$$T_p = 0.7624T_m + 17.0991 \quad (1)$$

For HTU31,

$$RH_p = 0.6433RH_m + 16.489 \quad (2)$$

For Pressure,

$$P_p = 0.5275P_m + 498.38 \quad (3)$$

where T_p, RH_p and P_p are the predicted temperature, relative humidity and pressure, while T_m, RH_m and P_m are the measured temperature, relative humidity and pressure. A correlation analysis was conducted, resulting in a correlation coefficient of 0.8324 for relative humidity, 0.9827 for temperature, and 0.9519 for pressure between the developed and standard devices. In addition, the signal strength of the GSM/GPRS device was correlated with a Galaxy A10s. Table 3 shows the received signal strength measurements taken at the Postgraduate Physics Laboratory, the Federal University of Technology, Akure, Nigeria at 10-minute intervals. The correlation coefficient between the devices is close to unity (0.99), indicating a strong agreement. The signal strength received between the two devices show no noticeable distinction based on the ANOVA test as presented in Table 4. The p-value of 0.93 is higher than the significance level (α) of 0.05, suggesting no statistically significant variance.

3.3. Statistical Validation

To prove the validity of the analytical method, statistical analysis of the data collected during the validation was also presented. The computation of the correlation (R^2), root mean square error (RMSE), mean absolute error (MAE), and standard deviation (S.D) are the main variables utilized for the interpretation of the results of analytical technique validation. Correlation (R^2) was estimated using:

$$R^2 = 1 - \frac{RSS}{TSS} \quad (4)$$

where R^2 is the coefficient of determination, RSS is the sum of squares residual and TSS is the total sum of squares.

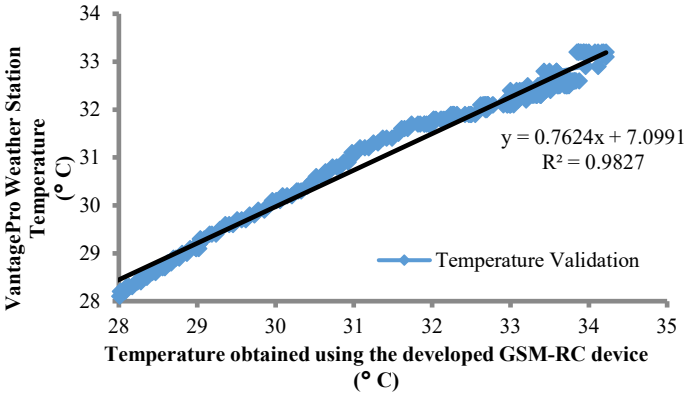

Figure 3: The validation of the temperature for the GSM-RC Device with Vantage Pro Weather Station

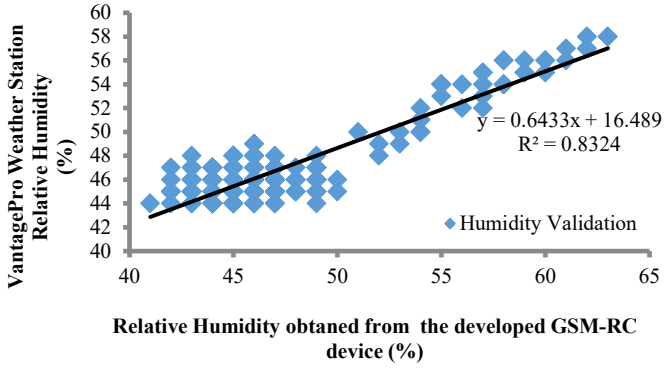

Figure 4: The validation of the relative humidity of the GSM-RC Device with Vantage Pro Weather Station

Table 2: Data obtained from the developed measuring device during the performance evaluation

Time	Signal Quality	Signal Strength (dBm)	Sat. View	Sat. Used	Lat. (°)	Long. (°)	Temp. (°C)	RH (%)	Pressure (mbar)	Heat Index (°C)	Radio Refractivity (N-units)
23:26:30	11	-92	8	7	7.2989	5.1343	27	53	968.11	27.60	328.52
23:26:56	11	-92	9	8	7.2989	5.1343	27	53	968.08	27.60	328.51
23:27:24	11	-92	8	7	7.2989	5.1343	27	53	968.14	27.60	328.53
23:27:53	11	-92	8	7	7.2989	5.1343	27	53	968.07	27.60	328.51
23:28:19	11	-92	8	8	7.2989	5.1343	27	53	967.98	27.60	328.49
23:28:45	10	-94	7	7	7.2989	5.1343	27	53	968.08	27.60	328.51
23:29:13	10	-94	8	7	7.2989	5.1343	27	53	968.02	27.60	328.50
23:29:43	10	-94	9	6	7.2989	5.1343	27	52	968.08	27.54	327.04
23:30:12	10	-94	9	7	7.2989	5.1343	27	53	968.07	27.60	328.51
23:30:41	10	-94	9	8	7.2989	5.1343	27	53	968.04	27.60	328.50
23:31:09	11	-92	8	8	7.2989	5.1343	27	53	968.06	27.60	328.51
23:31:35	10	-94	9	8	7.2989	5.1343	27	53	968.00	27.60	328.49
23:32:02	11	-92	10	9	7.2989	5.1343	27	53	968.08	27.60	328.51
23:32:29	11	-92	9	8	7.2989	5.1343	27	53	968.06	27.60	328.51
23:32:55	10	-94	9	8	7.2989	5.1343	27	53	967.93	27.60	328.47
23:33:23	10	-94	7	6	7.2989	5.1343	27	53	967.95	27.60	328.48
23:33:51	11	-92	8	7	7.2989	5.1343	27	53	967.94	27.60	328.48
23:34:19	10	-94	9	8	7.2989	5.1343	27	53	967.92	27.60	328.47
23:34:48	10	-94	9	8	7.2989	5.1343	27	53	967.95	27.60	328.48
23:35:15	10	-94	9	8	7.2989	5.1343	27	53	967.88	27.60	328.46
23:35:44	11	-92	8	8	7.2989	5.1343	27	53	967.92	27.60	328.47
23:36:11	11	-92	9	8	7.2989	5.1343	27	53	967.94	27.60	328.47
23:36:39	11	-92	8	7	7.2989	5.1343	27	53	967.93	27.60	328.47
23:37:06	11	-92	9	8	7.2989	5.1343	27	53	967.97	27.60	328.48
23:37:34	10	-94	9	8	7.2989	5.1343	27	53	967.89	27.60	328.46
23:38:03	11	-92	8	7	7.2989	5.1343	27	53	967.98	27.60	328.49
23:38:32	9	-96	9	8	7.2989	5.1343	27	53	967.87	27.60	328.46
23:39:00	11	-92	8	7	7.2989	5.1343	27	53	967.88	27.60	328.46

Table 3: Comparison of the received signal strength between the GSM-RC and Samsung Galaxy A10s.

Time interval (minutes)	GSM-RC RSS (dBm)	Samsung Galaxy A10s RSS (dBm)
0	-80	-79
10	-80	-79
20	-70	-71
30	-72	-71
40	-56	-56
50	-76	-75
60	-76	-76
70	-74	-74
80	-66	-67
90	-65	-66
100	-77	-78
110	-73	-74
120	-61	-63
	correlation	0.992291

Table 4: The ANOVA results of the signal strength received between GSM-RC and Galaxy A10s

ANOVA: Single Factor						
OUTPUT						
Groups	Number	Addition	Mean	Variance		
GSM-RC device	13	-926	-71.2308	54.02564		
Galaxy A10s	13	-929	-71.4615	46.9359		
ANOVA trend	SS	diff	MS	F	P-value	F crit
Between Groups	0.346154	1	0.346154	0.006857	0.934691	4.259677
Amidst Groups	1211.538	24	50.48077			
Summation	1211.885	25				

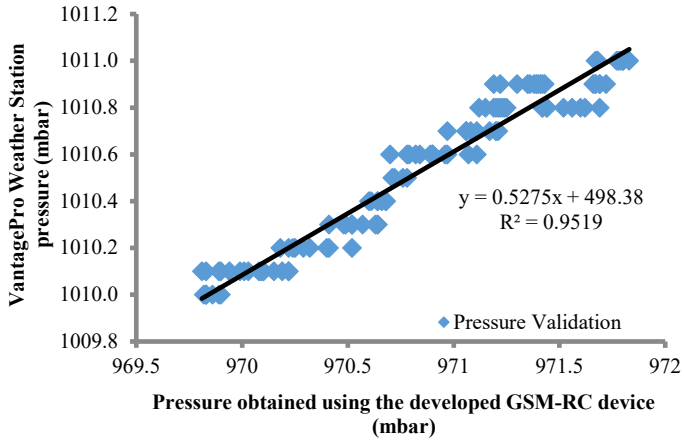

Figure 5: The validation of the pressure for the GSM-RC Device with Vantage ProWeather Station

The Root Mean Square Error (RMSE) was estimated using:

$$RMSE = \sqrt{\frac{\sum(x_i - \hat{x}_i)^2}{N}} \quad (5)$$

where RMSE is the root mean square error, x_i is the actual observation of time series, $\hat{x}_i$ is the estimated time series and N is the number of non-missing data points. The Mean Absolute Error (MAE) was also calculated using:

$$MAE = \frac{\sum|y_i - x_i|}{n} \quad (6)$$

where MAE is the mean absolute error, y_i is the prediction, x_i is the true value and n is the total number of data points.
The standard Deviation (S.D) was calculated using:

$$S = \sqrt{\frac{\sum(x_i - \bar{x})^2}{n-1}} \quad (7)$$

where x_i is the actual observation, $\bar{x}$ is the mean and n is the total number of observations. A statistical software programme was used to carry out these calculations. Table 5 shows the result obtained from the statistical validation of the radio climatological parameters between the VantagePro weather station and the developed device.

Table 5: Statistical validation of measured data for Radio climatological parameters between the developed GSM-RC device and the Standardize Vantage Pro

Parameters	R^2	RMSE	MAE	S.D
Temperature (T)	0.983	0.181	2.499	3.144
Relative Humidity (RH)	0.832	0.350	5.391	9.994
Pressure (P)	0.957	1.917	4.917	1.554

3.4. Seasonal analysis of the measurement obtained from the Field

This section discusses the seasonal analysis of the data obtained using the developed device. Each of the weekly hourly variables was averaged and presented for comparison over the months of the year. GSM signal strength, temperature, and relative humidity were accessed and further evaluated to establish the relationship between them. April, July, and January were chosen to represent the commencement, intense, and dry seasons, respectively. For the MTN network during the commencement of the rainy season, intense rainy season, and dry season, the GSM signal strength was correlated with the temperature, pressure, and relative humidity

3.5. Influence of Atmospheric parameter on RSS during the commencement of rainy season (April)

The correlation among signal strength, temperature, humidity, and pressure on a typical day in April is shown in Figures 6 (a–c). Data gathered daily was used to analyze the information for 24 consecutive hours. Since the correlation follows the same pattern, only the reading taken on April 1, 2022, is presented. Figure 6a shows that while the relative humidity profile is high at night, the values begin to decline in the middle of the day. In Figure 6b, during the day, temperatures typically oscillate, which can cause changes in atmospheric pressure. As observed in the morning hours (Figure 6b), when the temperatures are cooler, atmospheric pressure is higher than during the hot afternoon hours when the air is less dense. Similarly, at night, when temperatures cool again, atmospheric pressure tends to increase. In the early hours, as shown in Figures 6a and 6c, the humidity is high but the pressure profile is low. This could be influenced by the fact that water molecules are higher than oxygen and nitrogen molecules, which are the primary components of the atmosphere. As the amount of water vapor in the air (humidity) increases, the air becomes less dense, which may lead to a decrease in atmospheric pressure observed during those hours [11].

It was also observed that there are empirical relationships between the GSM signal strength, temperature, relative humidity, and pressure. The empirical correlations between the RSS, temperature, relative humidity, and pressure are presented in Table 6. The developed linear relationships are:

$$RSS_T = m_1 T + C_1, \quad (8)$$

for signal strength in dBm and temperature in °C;

$$RSS_{RH} = m_2 RH + C_2 \quad (9)$$

for signal strength and relative humidity in %; and

$$RSS_P = m_3 P + C_3 \quad (10)$$

for signal strength and pressure in mbar

Generally, the results presented in Table 6 show very weak correlations between signal strength, temperature, relative humidity, and pressure. It also shows a varying positive and negative correlation for each of the examined days in April. Previous researchers have also examined the variance or correlation between signal strength and meteorological parameters [3], [12-13]. The degree of linear dependence of GSM

RSS on temperature, relative humidity, and pressure has also been quantified using the Pearson correlation coefficient to provide a better understanding.

On signal strength, temperature has a small but significant impact except for the third and fifth days, which are positive, with all the relationships showing a linear, negative trend. In terms of impact size, there are various variances as well (regression coefficient). As presented in Table 6, there is a low and negative correlation between GSM RSS and temperature, while the correlation coefficient varies. This could be due to the characteristics of the measurement site, as reported by [14], [15], and [16]. Additionally, on the selected days, the GSM RSS was correlated with the temperature.

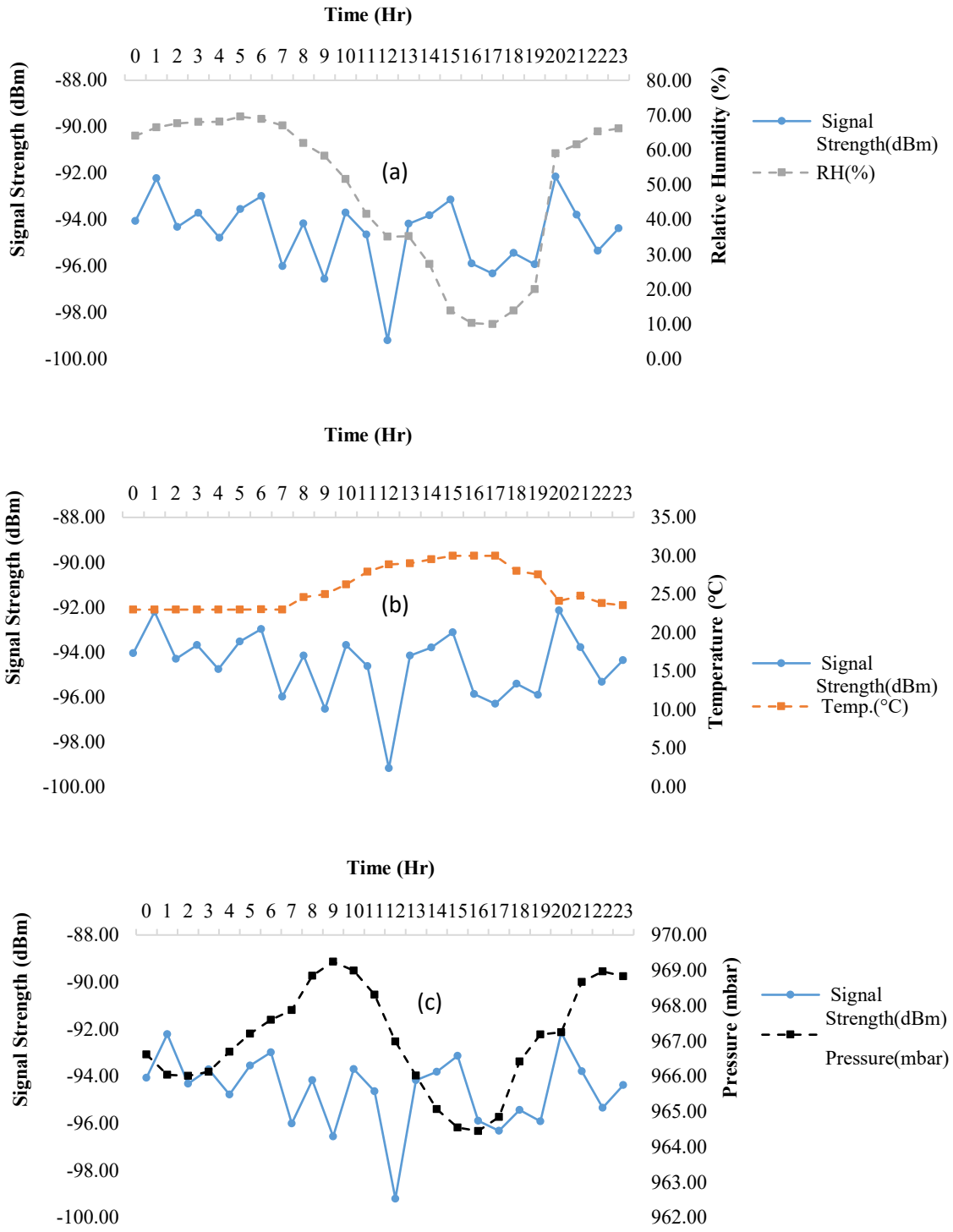

Figure 6: Mean hourly variation of GSM signal strength with (a) relative humidity (b) temperature and (c) pressure on a typical day (01-04-2022)

Table 6: Empirical correlation between GSM RSS and the selected atmospheric parameters

Days	T, RH and Pressure regressed on RSS	Slope (m_1,m_2 and m_3)	Intercept (c_1,c_2 and c_3)	correlation, coefficient, r
01-04-22	T	-0.2120	-37.829	-0.3774
	RH	0.0260	-95.859	0.3661
	Pressure	-0.0537	-42.7110	-0.0510
02-04-22	T	-0.0319	-90.594	-0.0646
	RH	0.0076	-91.761	0.1268
	Pressure	0.2515	-335.000	0.2818
03-04-22	T	0.4298	-102.201	0.2803
	RH	-0.0741	-87.930	-0.4089
	Pressure	-0.6151	503.459	-0.3353
04-04-22	T	-0.2091	-89.853	-0.2052
	RH	0.0223	-95.895	0.1724
	Pressure	0.5051	-583.801	0.3544
05-04-22	T	0.1562	-96.942	0.2115
	RH	-0.0207	-92.111	-0.2664
	Pressure	-0.0740	-21.4267	-0.0593
06-04-22	T	-0.0870	-90.189	-0.1138
	RH	0.0085	-92.768	0.1049
	Pressure	-0.4817	-379.316	-0.3722
07-04-22	T	-0.4309	-84.147	-0.4159
	RH	0.0543	-97.575	0.4912
	Pressure	0.2245	-312.466	0.1504

The third and fifth days, which have positive and low network correlation values, are an exception. For the selected days in April 2022, there is a weak but positive correlation between relative humidity and GSM RSS. This indicates that there may be additional parameters influencing it as it varies and may probably be caused by the humid nature of the season as reported in the work of [14] and [15]. GSM RSS and relative humidity exhibit a very weak negative correlation on the third and fifth days. Pressure when correlated with GSM RSS shows a very low correlation for the first, fifth and seventh days while the second, third, fourth and sixth days show a moderate correlation.

The peak (maximum) and dip (minimum) trend of the GSM RSS data are also shown in Table 7 together with the temperature, relative humidity, and pressure. Table 7 shows that the signal strength fluctuates for the network, having its maximum and minimum values between -87.14 (03-04-22) and -102.50 (03-04-22). Similar to this, analogue temperature and relative humidity variations were converted to digital values to obtain their

corresponding varying values. For temperature, the peak and least values were 31.99 °C (02-04-2022) and 22.70 °C (06-04-2022). Humidity has peak values of 74.80% (07-04-2022) and a least value of 9.00 (02-04-2022 and 03-04-2022) while pressure has a peak value of 971.29 mbar (02-04-2022) and a dip value of 962.49 mbar (03-04-2022). In particular, 07-04-2022 has the least value for temperature, and the highest peak value for humidity, and the signal strength fluctuation is significant. This might be due to the transition from the dry to the wet seasons, when the atmosphere gradually becomes moister as the temperature drops, the humidity value increases. This might prompt scattering of the radio signal and affects the signal quality.

3.6. Influence of Influence of Atmospheric parameter on RSS during Intense rainy season (July)

The correlation of signal strength with temperature, relative humidity, and pressure on a typical day during July is shown in Figures 7 (a–c). The analysis is done for 24 consecutive hours on intense rainy days. Since the correlation follows the same pattern, only the reading taken on July 1, 2022, is presented. The result presented in Figure 6a shows that the relative humidity profile is strong and essentially consistent during the chosen days. When it is foggy, daytime recorded data show that the humidity profile is often high because of the low temperature. The average temperature and humidity in cloudy climates are 27.73 °C and 84.04%, respectively, as presented in Figures 7a and 7b. This could be due to the decrease in temperature during the rainy season as there is an increase in cloud cover. As more clouds form in the atmosphere, they can reflect a greater amount of sunlight back into space, which can lead to a decrease in temperature at the Earth's surface. Additionally, as rain falls from the clouds, it can cool the air, leading to further decreases in temperature. At the same time, higher values of humidity were observed. This is due to the increase in moisture in the air, which is caused by several factors such as increased evaporation from bodies of water, increased transpiration from plants, and the influx of moist air masses from other regions. The implication is that during this condition, the nature of the radio signal will be weak due to the high humidity.

It was also observed that the GSM signal strength, temperature, relative humidity, and pressure all exhibit empirical connections, as presented in Table 8. The RSS, temperature (T), relative humidity (RH), and pressure (P) all showed a linear relationship in the result. The developed linear relationships are in agreement with equations (8)–(10).

For the selected days in July, Table 8 generally reveals very weak correlations between signal strength, temperature, relative humidity, and pressure. It also exhibits a periodic positive and negative correlation for each of the selected days. Based on the Pearson correlation coefficient, the linear dependence of the GSM RSS with temperature, relative humidity, and pressure was evaluated

The correlation between pressure and the RSS slightly varies with an increase in signal strength. As presented in Table 8, the first and second days show a negative trend, while the fifth, sixth, and seventh days show a linear but weak trend. The temperature values have a negligible but noticeable impact, as seen on the third day. Further analysis shows that except for the first day, which displays a weak negative correlation, other days show a weak positive trend. This is in agreement with the work of Christian and Michael [17], also in July. The implication is that the trend may be influenced by other factors due to the nature of the period [14-15]. Similarly, the sixth day in July has a positive link with the other days. However, on the second, third, and fourth days of the selected days, there exists a weakly negative correlation.

The temperature, relative humidity, and pressure are all displayed in Table 9, along with the peak and dip of the GSM RSS data. Table 9 shows that the signal strength fluctuates for the network, with a peak value at -89.11 (04-07-22) and the least value at -96.46 (02-07-22).

Similar to this, analog temperature and relative humidity variations were converted to digital values to obtain their corresponding varying values. For temperature, it has its peak value at 29.96 °C (07-04--2022) and its least value, at 24.20 °C (07-01--2022), while relative humidity has its peak value at 89.40 % (01-07--2022) and the least at 69.65 (02-07--2022 and 05-07-2022).

For pressure, the peak was observed at 973.37 mbar (06-07-2022) and the least value at 968.70 mbar (04-07-2022). The highest peak value of the GSM RSS, the least temperature value, the peak relative humidity value, and the lowest pressure value were all observed on July 4, 2022, in particular. This could be due to the consistent increase in atmospheric moisture as the rainy season intensifies and the temperature decreases. Another reason could be as a result of relative humidity, which is constantly higher during the rainy season than actual rainfall.

3.7. Influence of atmospheric parameters on RSS during the dry season (January)

The correlation of signal strength with temperature, relative humidity, and pressure on a typical day during January is also shown in Figures 8 (a–c). The information in Figures 8 (a–c) was analyzed using data that was collected for 24 consecutive hours daily. Figures 8a and 8b show that the relative humidity profile is at its minimum and the temperature profile is at its maximum on the chosen days. This could be related to how the earth responds to solar insolation, which is a primary driving force behind the weather conditions that were being experienced when the Harmattan season was at its peak. Since the moisture content is lower during this time, light will move at a faster rate [18]. The Harmattan season is connected to the northeasterly wind that crosses the Sahara Desert while there is a dry climate [19]. Another factor that can cause an increase in temperature during the dry season is the absence of rain or cloud cover. As there is little to no precipitation, the sun's energy is able to penetrate the atmosphere more directly, which can lead to a greater amount of solar radiation being absorbed at the Earth's surface. This could result in higher temperatures, particularly in regions with a high incidence of sunlight. At the same time, the dry season is characterized by a decrease in humidity. This is because there is little to no moisture in the air, and there is little to no precipitation to introduce moisture into the atmosphere. Additionally, any moisture that is present may be quickly evaporated due to the high temperatures and low relative humidity.

Table 7: Summary of variation of GSM RSS and Radio climatological parameters during the Commencement of rainy season (April).

	Signal Strength (dBm)		Temperature (°C)		Humidity (%)		Pressure (mbar)	
Day	Highest Peak	Dip	Highest Peak	Dip	Highest Peak	Dip	Highest Peak	Dip
01-04-22	-92.15	-99.20	30.00	23.00	69.54	10.03	969.24	964.45
02-04-22	-89.45	-94.27	31.99	23.00	67.00	9.00	971.29	965.69
03-04-22	-87.14	-102.50	31.46	24.33	59.57	9.00	969.61	962.49
04-04-22	-91.08	-99.35	28.71	23.00	61.77	11.10	970.78	965.57
05-04-22	-90.82	-97.00	29.43	23.00	67.66	11.03	970.25	966.22
06-04-22	-90.62	-97.25	29.43	22.70	67.05	11.24	970.33	966.08
07-04-22	-91.44	-100.37	30.79	22.99	74.80	9.85	970.73	964.63

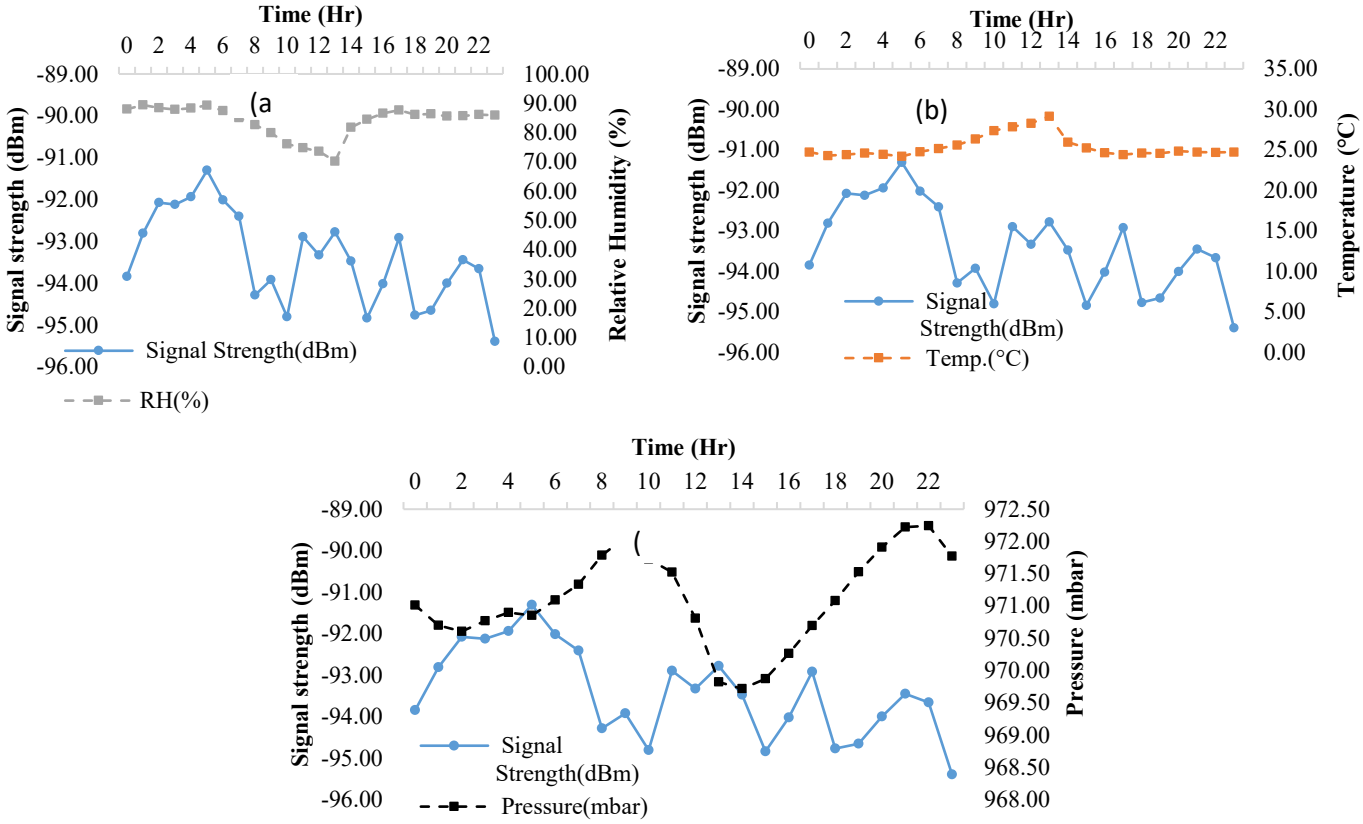

Figure 7: Mean hourly variation of GSM signal strength with (a) relative humidity (b) temperature (c) pressure on a typical day (01-07-2022)

Table 8: Empirical correlation between GSM RSS and the selected atmospheric parameters

Days	T, RH and Pressure regressed on RSS	Slope (m_1,m_2 and m_3)	Intercept (c_1,c_2 and c_3)	correlation, coefficient, *r*
01-07-22	T	-0.0730	-91.550	-0.0924
	RH	0.0371	-96.526	0.1809
	Pressure	0.6923	290.609	-0.2662

02-07-22	T	0.1984	-99.374	0.3053
	RH	-0.0702	-88.399	-0.3668
	Pressure	-0.2381	137.209	-0.2726
03-07-22	T	0.9808	-118.947	0.4130
	RH	-0.0353	-89.278	-0.0614
	Pressure	-0.3343	232.636	-0.2069
04-07-22	T	0.0398	-91.254	0.0734
	RH	-0.0529	-86.017	-0.3016
	Pressure	-0.1069	13.584	-0.1565
05-07-22	T	-0.1861	-87.137	-0.1277
	RH	0.0973	-99.985	0.1566
	Pressure	0.0669	-157.115	0.0350
06-07-22	T	-0.7069	-73.671	-0.4410
	RH	0.2318	-111.378	0.4203
	Pressure	-0.0413	-52.352	-0.0303
07-07-22	T	0.0092	-92.408	0.0138
	RH	0.0074	-92.763	0.0310
	Pressure	0.0319	-123.132	0.0446

Table 9: Summary of variation of GSM RSS and Radio climatological parameters during the intense rainy season (July).

	Signal Strength (dBm)		Temperature (°C)		Humidity (%)		Pressure (mbar)	
Day	Highest Peak	Dip	Highest Peak	Dip		Highest Peak	Dip	Highest Peak
01-07-22	-91.31	-95.40	29.17	24.20	01-07-22	-91.31	-95.40	29.17
02-07-22	-92.33	-96.46	29.62	24.50	02-07-22	-92.33	-96.46	29.62
03-07-22	-89.56	-95.74	28.86	26.33	03-07-22	-89.56	-95.74	28.86
04-07-22	-89.11	-91.74	29.96	26.45	04-07-22	-89.11	-91.74	29.96
05-07-22	-89.43	-95.67	28.81	25.60	05-07-22	-89.43	-95.67	28.81
06-07-22	-90.00	-96.19	28.93	25.33	06-07-22	-90.00	-96.19	28.93
07-07-22	-91.14	-94.31	28.47	24.87	07-07-22	-91.14	-94.31	28.47

Also in Figure 8a, the variation of GSM signal strength did not correlate with the low relative humidity readings that were recorded on this day. This could be due to the Harmattan dust haze and other pollutants in the atmosphere during this month. Moreover, attenuation by scattering is greater for relatively large wavelengths of GSM signal strength compared to dust particle size, which might disturb the atmosphere and radio wave propagation. This is consistent with the findings by [19] and earlier researchers who also observed radio signal obstruction during Harmattan and an absence of radio line-of-sight [20-22]. Since the correlation follows the same pattern, only the reading taken on January 1, 2022, is fully discussed. For the selected days in January, Table 10 generally reveals moderate correlations between signal strength, temperature, relative humidity, and pressure. It also exhibits a periodic positive and negative correlation for each of the selected days. Based on the Pearson correlation coefficient, the linear dependence of the GSM RSS with temperature, relative humidity, and pressure was evaluated. As the RSS increases, the correlation between pressure and RSS declines with slight changes. As shown in Table 10, the relationship between pressure and RSS was positively linear and moderate on the second and seventh days, except for the other days, which were weak. Apart from the first day (onset), temperature and humidity show a clear link with RSS throughout the days. Possibly, this was influenced by how the planet reacts to solar insolation, which is a major cause of the weather that was present. Further analysis shows that except for the third day, when the humidity had a positive but relatively moderate correlation with RSS for all the selected days, there was a negative but moderate correlation between temperature and RSS across the selected days. Nonetheless, different correlation coefficient values can exist, as reported by [14], [16], and [23].

Table 11 shows that the signal strength fluctuates for the network, with the peak value and least value between -52.00 dBm (06-01-22 and 07-01-2022) and -104.67 dBm (01-01-22), respectively. Similar to this, analog temperature and relative humidity variations were converted to digital values to obtain their corresponding varying values. For temperature, its peak value was observed at 36.16 °C (06-01-22 and 07-01-2022), and the least value was 22.11 °C (04-01-2022). The highest peak value for relative humidity was noticed at 87.82% (06-01-22 and 07-01-2022), and the least value was 07.24 (05-01-2022). For pressure, its peak value was 973.05 mbar (01-01-2022) and its dip was 965.94 mbar (05-01-2022). The study discovered that on the selected days in January, this season is characterized by high temperatures (36.16°C) and low relative humidity values (7.24%). This could be as a result of the Harmattan period, during which the amount of atmospheric moisture decreases and the temperature of the environment rises. Also, these could be linked to the way the planet reacts to the amount of solar radiation that strikes the earth's surface as electromagnetic energy, which is a significant factor in the weather conditions observed. Since the moisture content is lower during this time, light will move at a faster rate. This could explain the peak value experienced for signal strength (-52.00 dBm) during the season.

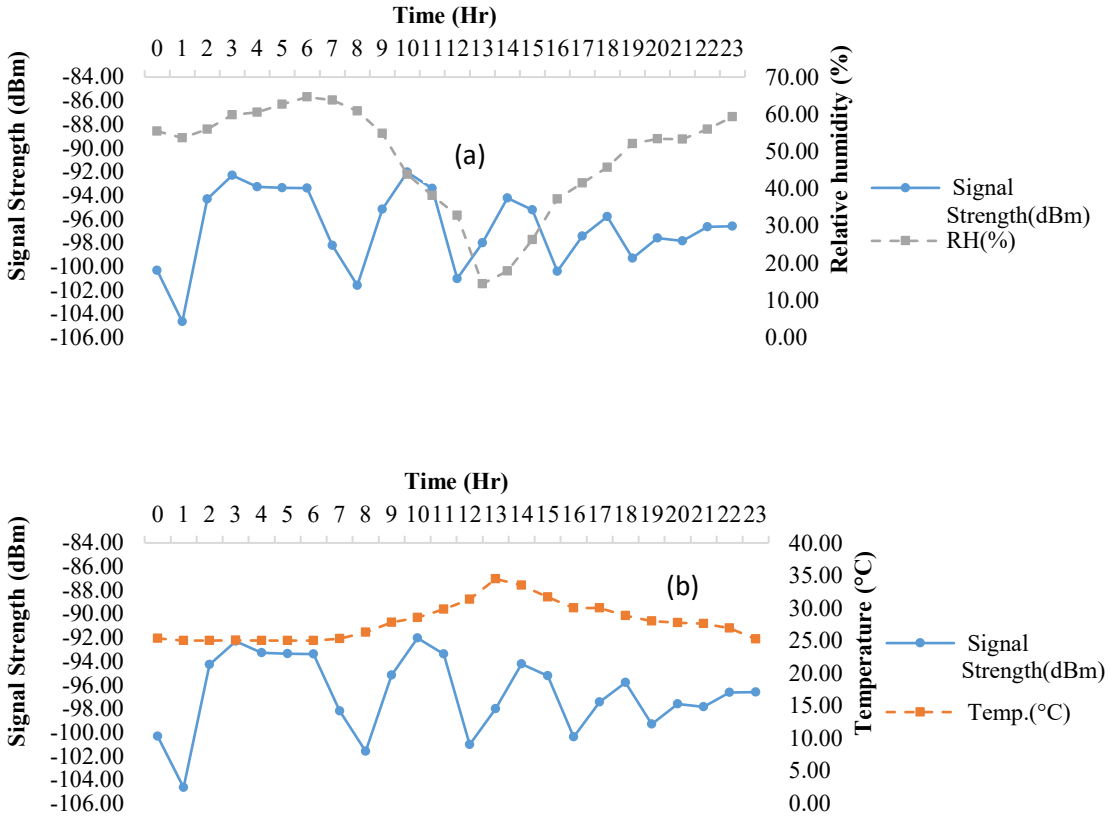

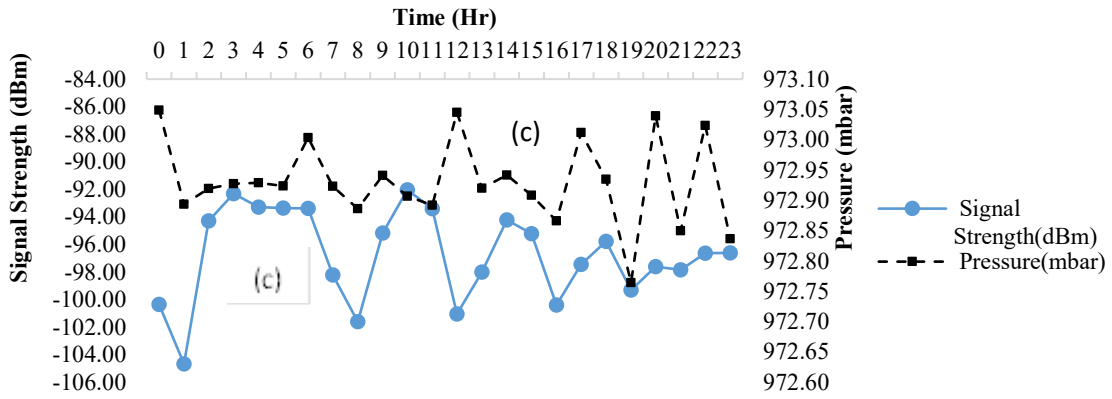

Figure 8: Mean hourly variation of GSM signal strength with (a) relative humidity (b) temperature (c) pressure on a typical day (01-01-2022)

Table 10. Empirical correlation between GSM RSS and the selected atmospheric parameters

Days	T, RH and Pressure regressed on RSS	Slope (m_1,m_2 and m_3)	Intercept (c_1,c_2 and c_3)	correlation, coefficient, r
01-01-22	T	-0.0415	-95.6028	-0.0361
	RH	0.0090	-97.1964	0.0391
	Pressure	1.4132	-1471.80	0.0301
02-01-22	T	-2.6253	-10.1192	-0.4670
	RH	0.1975	-87.5551	0.4336
	Pressure	3.8263	-3787.00	0.5734
03-01-22	T	0.7956	-98.0658	0.3890
	RH	-0.0811	-74.1352	-0.4094
	Pressure	-0.6970	597.890	-0.2190
04-01-22	T	-0.8650	-70.6787	-0.3681
	RH	0.1118	-98.4487	0.3480
	Pressure	-0.4120	305.883	-0.0660
05-01-22	T	-0.3410	-86.8400	-0.4880
	RH	0.0544	-98.4200	0.4960
	Pressure	0.2199	-309.200	0.1258
06-01-22	T	-0.5695	-40.6099	-0.6886
	RH	0.1389	-66.7231	0.6630
	Pressure	-0.0110	-46.8500	-0.0040
07-01-22	T	-0.2548	-48.2391	-0.3328
	RH	0.0744	-60.7671	0.3863
	Pressure	1.7714	-17772.9	0.5807

Table 11: Summary of variation of GSM RSS and Radio climatological parameters during the intense rainy season (July).

	Signal Strength (dBm)		Temperature (°C)		Humidity (%)		Pressure (mbar)	
Day	Highest Peak	Dip	Highest Peak	Dip	Highest Peak	Dip	Highest Peak	Dip
01-01-22	-92.04	-104.67	34.47	25.00	64.63	14.40	973.05	972.76
02-01-22	-66.37	-104.50	29.00	24.43	57.85	10.73	970.73	966.66
03-01-22	-69.43	-82.51	30.00	23.50	62.37	09.00	971.24	967.41
04-01-22	-71.66	-100.45	32.05	22.11	77.45	08.95	972.04	968.39
05-01-22	-88.61	-99.79	33.99	23.00	68.77	07.24	971.75	965.94
06-01-22	-52.00	-62.55	36.16	24.69	87.82	41.48	971.67	967.64
07-01-22	-52.00	-62.40	36.16	24.63	87.82	41.48	971.16	967.64

4. Conclusion

This work has developed a handy and locally-based device that can simultaneously measure the received signal strength and atmospheric parameters, rather than the cumbersome method of measuring them individually. The global system for mobile communication received signal strength and radio climatological measuring devices has been successfully developed. A statistical analysis of the received level of signal between the GSM-RC and the Samsung Galaxy A10s mobile reveals a correlation of roughly 0.99. The results of an ANOVA analysis of variance demonstrate that there is not a noticeable distinction between the signal strength values from the developed and conventional devices. The P (value) is determined to be 0.93 and higher α (value) of 0.05. The values obtained were in good agreement with those obtained using a standard device. The developed instrument, which was validated against the standard device, measured relative humidity and temperature, with their accuracy close to unity. A field test using this device shows some correlations between the radio-climatological parameters for some selected seasons and the GSM RSS. The findings indicate a weak and poor correlation between temperature and GSM signal strength, while relative humidity and pressure are positive but weak correlation. RSS has the highest value during the dry season (January), when the atmosphere is mostly perturbed, while temperature variation is low in July and high in January. Pressure and humidity attained their peak values during the intense rainy season (July) and their lowest values during the dry season (January). The implication of this is that the pressure and susceptibility of the radio signal to losses increase with increasing humidity at the study location. The developed device has been found to be cheap, handy, and user-friendly.

Conflict of Interest

All authors declare no conflict of interest in this paper.

References

[1] J. S Ojo, A. Ayegba, A.T Adediji "Impact of Atmospheric Parameters and Noise Temperature on Digital Terrestrial Television Signal Strength over Karshi Area, Abuja, North-Central, Nigeria", IOP Conference Series: Earth and Environmental Science, 2021, **doi:** 10.1088/1755-1315/665/1/012048

[2] J. J. Popoola, I.O Megbowon, V.S Adeloye V. S. (2009). Performance Evaluation and Improvement on Quality of Service of Global System for Mobile Communications in Nigeria. Journal of Information Technology Impact (JITI), **118**, 52–60, 2009.

[3] U. U Abraham., U.O Okpo., E.O Elijah. "Instantaneous GSM signal strength with weather and environmental factors". Amer J Eng Res: **4**, 104-115, 2015.

[4] A. M. Zungeru, M. S. Ahmed, G. M Doko, D. Abdul-Azeez. "Modelling and Development of A Frequency Modulated Field Strength Indicator" International Journal of Emerging Trends in Engineering and Development, **1(4)**, 192-205, 2014

[5] L. Angrisani, D. Petri, M. Yeary, "Instrumentation and Measurement in Communication Systems". IEEE Instrumentation and Measurement Magazine, **18**(2), 4–10. 2015, DOI: 10.1109/MIM.2015.7066676

[6] B.L. Therajar, A.K Theraja, A testbook of elctrical technology. S. Chand & Company Ltd& Ram Nagar, New Dehli, 2005.

[7] M. H. Weik,. Communications Standard Dictionary, 2nd Edition, New York, NY, USA: Van Norstrand Reinhold Company Inc , 1983.

[8] M. Beigl, C. Henning, T. R. Roth-Berghofer, A. Kofod-Petersen, K. R. Coventry, H. R. Schmidtke "Modeling and Using Context". Procedings 7th International and Interdisciplinary Conference, CONTEXT 2011, Karlsruhe, Germany, September 26-30, 2011..

[9] G. F. Sa,. Lessons Learned from Smart Machines-CTIC-UNI Program for Developing for Capacity Building in Peruvian Undergraduates and Perspectives in The Near Future. mart Machines-CTIC-UNI Program, 2021.

[10] D. C Marubin, S. S Yi, "Development of Appropriate Power Distribution Design for Can-Sized satellite CanSAT" Journal of Advanced Industrial Technology and Application, **2(2),** 1-10, 2021.

[11] L. Ali, I. Alam, S. A. A. Shah, M. Yaqoob, "Various Meterological Parameters Effect on GSM Radio Signal Propagation for a Moderate Area", International Conference on Frontiers of Information Technology. 115-120, 2017, DOI: 10.1109/FIT.2017.00028

[12] B. G Ayatunji**,** B. Musa, H. Mai-Unguwa, L. A Sunmonu, A. S Adewumi, A. Sa'ad L Kado A, "Atmospheric humidity and its implications on UHF signal over Gusau, North West, Nigeria", Int J Sc Eng Res: **9**, 599-611, 2018..

[13] J. Amajama 2016. "Impact of atmospheric temperature on UHF radio signal" . Int J Eng Res Gen Sc: **4**, 619-622

[14] j. Luomal, I. Hakala,.. "Effects of Temperature and Humidity on Radio Signal Strength in Outdoor Wireless Sensor Networks". Computer Science and Information Systems, **5**, 1247-1255, 2015. doi:: https://doi.org/10.15439/2015F241

[15] K.E Ukhurebor, O. J, O. I Umukoro "Influence of meteorological variables on UHF radio signal: recent findings for EBS, Benin City, South-South, Nigeria". 2nd Int Conf Sc Sust Dev, IOP Conf. Series: Earth and Enviro Sc:

pp. 179, 2018.

[16] S. Sabu, S. Renimol, D. Abhiram, B. Premlet, "A study on the effect of temperature on cellular signal strength quality". 2017 International Conference on Nextgen Electronic Technologies: Silicon to Software (ICNETS2), 38-4, 2017. .

[17] S. A Christian U. O Michael. "Design and Construction of Weather Instrument and Its Use in Measurements to Determine the Effects of Some Weather Parameters on GSM Signal Strength". Advances in Applied Sciences. **6 (4)**, 142-154, 2021.

[18] O. L Ojo. "Geo-spatial distribution of radio refractivity and the influence of fade depth on microwave propagation signals over Nigeria", International Journal of Physical Science (Academic Journal) , **18(3)**, 72-83 , July 2023. doi.org/10.5897/IJPS2023.5036.

[19] D. Dajab, "Perspectives on the effects of harmattan on radio frequency waves". Journal of Applied Sciences Research, **2(11)**, 1014-1018, 2006.

[20] M. U. Onuu, A. Adeosin "Investigation of propagation characteristics of UHF waves in Akwa Ibom State, Nigeria". Indian J Rad Space Phy: **37,** 197-203, 2008

[21] A Eyo, O. E., Menkiti, A. I., Udo, S. O.. "Microwave signal attenuation in Harmattan weather along Calabar-Akamkpa line-of-sight link". Turk J Phys: **27**, 153-160, 2003..

[22] A. S Abdullahi. J. S Ojo, A. T Adediji, "Statistical Analysis of Atmospheric Parameters, Noise Temperature and Digital Terrestrial Television Signal Strength Over JOS Metropolis, Plateau State, Nigeria". July 2022 Heliyon 8(3):e09988

[23] L. Sa'du, N. C Maduka, A. Kado, I. Abdulmuninu, M. Bello. "Assessment of mobile network signal strength for GSM networks in Gusau, Zamfara State, Nigeria". Inter J Innov Sc, Eng Tech: **6**, 10-20, 2022.

Copyright: This article is an open access article distributed under the terms and conditions of the Creative Commons Attribution (CC BY-SA) license (https://creativecommons.org/licenses/by-sa/4.0/).